

Predicting the density-scaling exponent of a glass-forming liquid from Prigogine–Defay ratio measurements

Ditte Gundermann¹, Ulf R. Pedersen², Tina Hecksher¹, Nicholas P. Bailey¹, Bo Jakobsen¹, Tage Christensen¹, Niels B. Olsen¹, Thomas B. Schröder¹, Daniel Fragiadakis³, Riccardo Casalini³, C. Michael Roland³, Jeppe C. Dyre¹ and Kristine Niss¹*

Understanding the origin of the dramatic temperature and density dependence of the relaxation time of glass-forming liquids is a fundamental challenge in glass science. The recently established ‘density-scaling’ relation quantifies the relative importance of temperature and density for the relaxation time in terms of a material-dependent exponent. We show that this exponent for approximate single-parameter liquids can be calculated from thermoviscoelastic linear-response data at a single state point, for instance an ambient-pressure state point. This prediction is confirmed for the van der Waals liquid tetramethyl-tetraphenyl-trisiloxane. Consistent with this, a compilation of literature data for the Prigogine–Defay ratio shows that van der Waals liquids and polymers are approximate single-parameter systems, whereas associated and network-forming liquids are not.

Many liquids are known to exhibit peculiar, sometimes even spectacular behaviour. Water is a notorious example with its many intriguing anomalies^{1,2}. This raises the questions: Do liquids exist with ‘simple’ behaviour and what characterizes such behaviour? Based on theory and simulations, recent papers^{3–5} proposed such a class of liquids, ‘strongly correlating liquids’, which are approximate single-parameter liquids⁶. The possible existence of approximate single-parameter liquids^{7–15} has important implications, particularly for addressing long-standing fundamental questions related to the glass transition^{16–20}, but so far it has not been convincingly demonstrated in experiment.

In this paper we present an experimental test of a striking prediction for strongly correlating liquids, namely that the density-scaling exponent—characterizing how to scale density and temperature for different state points to have the relaxation times superpose onto a master curve^{21–24}—may be calculated from the equilibrium fluctuations at a single state point⁵. The equilibrium fluctuations are probed using the fluctuation–dissipation theorem, which relates linear-response functions to fluctuations. The experiments were performed on the van der Waals glass-forming liquid, tetramethyl-tetraphenyl-trisiloxane, which is a commercial silicone oil (DC704). The paper further presents a reinterpretation of the classical Prigogine–Defay ratio, showing that many other systems are strongly correlating, that is, approximate single-parameter liquids. All together these results suggest that van der Waals liquids are strongly correlating, confirming the long-held, general view that these are simpler than associated liquids. In contrast, network-forming liquids such as water, glycerol, or silica are much more complex.

Temperature and volume both play important roles for the viscous slowing down as the glass transition is approached from

above^{25,26}. The first measurements of viscosity under high pressure were published in 1949 by Bridgman²⁷, but only during the past decade has a substantial amount of data become available on the dynamics of viscous liquids at different pressures. The information comes mainly from dielectric spectroscopy, but inelastic neutron scattering and other experiments have also been performed under pressure (ref. 24 reviews the dynamics of glass-forming liquids under hydrostatic pressure). The most important experimental finding from high-pressure studies of liquid dynamics is probably density scaling, that is, the fact that the temperature (T) and density (ρ) dependences of the relaxation time for many liquids can be described in terms of the single scaling variable $\rho^{\gamma_{\text{scale}}}/T$ (refs 21–24), where γ_{scale} is the so-called density-scaling exponent. Density scaling applies, for example, for van der Waals liquids, but not for hydrogen-bonded liquids²⁸.

A simple explanation of density scaling can be given for strongly correlating liquids. These are characterized by near proportionality between the isochoric thermal equilibrium fluctuations of the virial W and the potential energy U (refs 3–5), the quantities that give the configurational parts of pressure and energy, respectively. That is, W and U are the terms resulting from the molecular interactions, which are added to the kinetic ideal gas terms. The total energy E is the kinetic energy K plus the potential energy U , and the pressure p is likewise an ideal gas term $Nk_B T/V$ plus the configurational part W/V :

$$E = K + U$$

$$pV = Nk_B T + W$$

Here V is the volume and N the number of particles. Both the virial and the potential energy fluctuate around their equilibrium

¹DNRF Centre ‘Glass and Time’, IMFUFA, Department of Sciences, Roskilde University, Postbox 260, DK-4000 Roskilde, Denmark, ²Department of Chemistry, University of California, Berkeley, California 94720-1460, USA, ³Chemistry Division, Naval Research Laboratory, Washington, District of Columbia 20375-5342, USA. *e-mail: kniss@ruc.dk.

values. At any given time the fluctuations are defined by $\Delta W(t) = W(t) - \langle W \rangle$ and $\Delta U(t) = U(t) - \langle U \rangle$ (Δ is here used in the standard meaning of statistical mechanics, whereas in the Prigogine–Defay ratio literature Δ denotes the difference between liquid and glass properties).

A strongly correlating liquid has ‘isomorphs’, which are curves in the phase diagram along which a number of properties in reduced units—including the dynamics—are invariant⁵. The isomorph concept implies density scaling: A strongly correlating liquid’s isomorphs obey the equation $\rho^{\gamma_{\text{isom}}}/T = \text{Const.}$, where γ_{isom} is determined from the near proportionality between virial and potential energy isochoric fluctuations, $\Delta W(t) \cong \gamma_{\text{isom}} \Delta U(t)$ (ref. 5). In particular, the reduced-unit relaxation time is a function of $\rho^{\gamma_{\text{isom}}}/T$. The predicted equality of the fluctuation exponent γ_{isom} and the density-scaling exponent γ_{scale} has been verified for a few computer-simulated liquids^{29,30}, but never tested experimentally. Such a test is very demanding, however, because it involves new and unique measurements of several frequency-dependent thermoviscoelastic response functions.

In this work we present the first test of this type. To do so we have chosen a liquid expected to be strongly correlating. It is known from computer simulations and theoretical considerations that liquids with simple Lennard-Jones-like interactions are strongly correlating, whereas liquids with directional bonds (for example, hydrogen bonds) are not^{3–5}. This is consistent with the experimental finding that van der Waals bonded liquids obey density scaling, whereas hydrogen-bonded liquids do not. It is important to keep in mind that strong *WU* correlation implies density scaling, whereas the opposite is not necessarily true. Density scaling might well hold for a larger class of liquids. However, at this point there are only theoretical predictions for the density scaling exponent of strongly correlating liquids.

As our test sample we have chosen the van der Waals glass-forming liquid tetramethyl-tetraphenyl-trisiloxane (DC704). We expect it to be strongly correlating because it has a very low dipole moment, which means that it is truly van der Waals bonded, while the dipole moment is large enough to give a good signal in the high-pressure dielectric measurements. DC704 is moreover chemically very stable and an excellent glass former.

Figure 1a shows the dielectric relaxation time, defined as the inverse angular loss-peak frequency, for DC704 as a function of density for different isotherms, as well as data taken at atmospheric pressure. pVT-data were used to calculate the density at each state point. Density scaling is demonstrated in Fig. 1b, showing that all data collapse onto a master curve when the reduced-unit relaxation time is plotted as a function of the scaling variable $\rho^{\gamma_{\text{scale}}}/T$. The $\gamma_{\text{scale}} = 6.2 \pm 0.2$ is an empirical fit parameter and the reduced-unit relaxation time $\bar{\tau}$ is given by $\bar{\tau} = C\rho^{1/3}T^{1/2}\tau$, where C is an arbitrary constant with no influence on the scaling (it only changes the numbers on the y -axis). The use of reduced units is theoretically correct, but the actual difference between using reduced units or absolute values is minimal in the supercooled region because the relaxation times vary over many orders of magnitude, whereas T only changes 30% and ρ even less. In fact, when we perform the scaling using absolute values of τ we find $\gamma_{\text{scale}} = 6.1 \pm 0.2$.

Turning now to the isomorph prediction, the near proportionality of the equilibrium fluctuations, $\Delta W(t) \cong \gamma_{\text{isom}} \Delta U(t)$, is consistent with the theoretical expression for γ_{isom} (the sharp brackets denote NVT ensemble averages)⁵

$$\gamma_{\text{isom}} = \frac{\langle \Delta W \Delta U \rangle}{\langle (\Delta U)^2 \rangle}$$

To calculate this quantity from linear thermoviscoelastic measurements we reason as follows. A characteristic feature of viscous liquids is timescale separation. Fluctuations of the

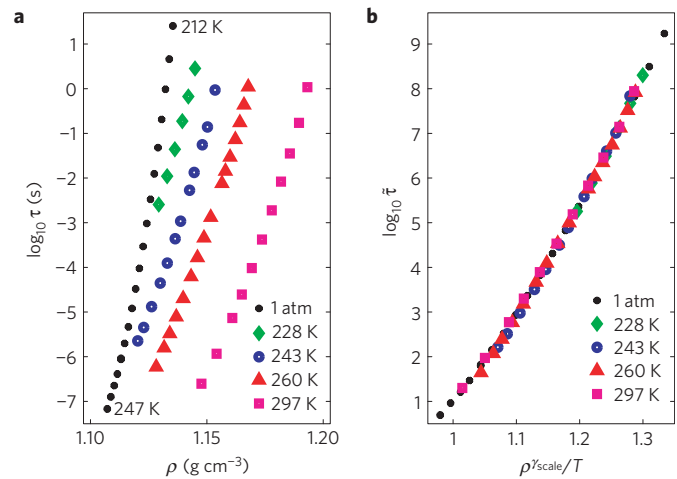


Figure 1 | The dielectric relaxation time τ measured along different isotherms and along the atmospheric pressure isobar for the silicone oil DC704. The points come from measured loss peaks and the relaxation times refer to inverse angular loss-peak frequencies. **a**, The relaxation times as functions of density (calculated from measured pVT-data). **b**, The reduced unit relaxation time, $\bar{\tau} = C\rho^{1/3}T^{1/2}\tau$, as a function of $K\rho^{\gamma_{\text{scale}}}/T$, where $\gamma_{\text{scale}} = 6.2 \pm 0.2$ is a parameter adjusted to collapse the data of **a**. C and K are constants which have no influence on the quality of the scaling; they only shift the axes.

kinetic terms decorrelate on a picosecond timescale. Consequently, if one averages the fluctuations in pressure and energy over a timescale much longer than picoseconds but much shorter than the liquid’s relaxation time, one gets the fluctuations of the configurational terms. For such averages it follows that $\langle \Delta W \Delta U \rangle / \langle (\Delta U)^2 \rangle \cong V \langle \Delta p \Delta E \rangle / \langle (\Delta E)^2 \rangle$. This brings us closer to something that can be accessed experimentally, because fluctuations in pressure and energy determine the thermoviscoelastic linear-response functions through the fluctuation–dissipation theorem: $V \langle \Delta p \Delta E \rangle / \langle (\Delta E)^2 \rangle = (\beta_V^{\text{slow}} - \beta_V^{\text{fast}}) / (c_V^{\text{slow}} - c_V^{\text{fast}})$, where $\beta_V = (\partial p / \partial T)_V$ is the pressure coefficient and c_V the isochoric specific heat per unit volume. Here ‘slow’ response means the long-time (low-frequency) liquid-like limit, and ‘fast’ response means the short-time (high-frequency) solid-like limit of the relevant (complex) frequency-dependent linear-response function of the equilibrium liquid, still probing the system at times much longer than phonon times. Thus

$$\gamma_{\text{isom}} = \frac{\beta_V(\omega \rightarrow 0) - \beta_V(\omega \rightarrow \infty)}{c_V(\omega \rightarrow 0) - c_V(\omega \rightarrow \infty)} \quad (1)$$

The high-frequency values ($\omega \rightarrow \infty$) correspond to solid-like responses, where the liquid has time to explore only one potential energy minimum, a so-called inherent state. This implies that γ_{isom} , as discussed later, can be evaluated approximately using the much easier measured values for the glassy state instead of the high-frequency values^{4,31}.

The two linear thermoviscoelastic response functions $\beta_V(\omega)$ and $c_V(\omega)$ refer to constant-volume measurements; experiments are usually performed under constant pressure, however. This problem can be overcome by measuring three independent thermoviscoelastic response functions and subsequently calculating $\beta_V(\omega)$ and $c_V(\omega)$ using standard thermodynamic relations. These relations include dynamic versions of the Maxwell relations, which are the so-called generalized Onsager reciprocity relations reflecting the time reversibility of the underlying microscopic equations of motion³². Unfortunately, even constant-pressure conditions are difficult to attain for ultra-viscous liquids because thermal expansion is often

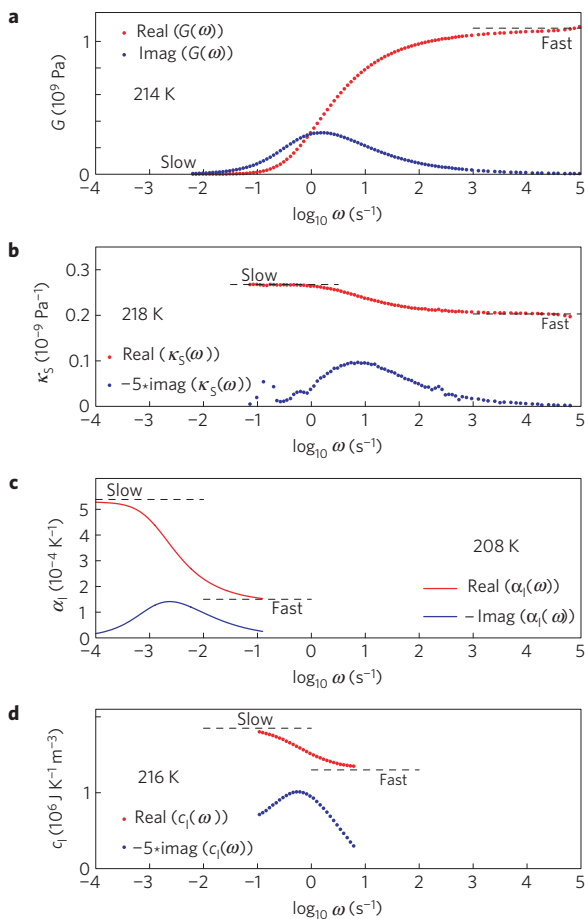


Figure 2 | Examples of frequency-dependent real and imaginary parts of the four required thermoviscoelastic response functions of DC704, illustrating the experimental challenges associated with checking the isomorph prediction $\gamma_{\text{scale}} = \gamma_{\text{isom}}$. The experimental techniques work in different frequency intervals (see the Methods section); to place the relaxation region central in the accessible frequency window for each technique we show data at temperatures that vary with response function. **a**, The shear modulus $G(\omega)$. **b**, The adiabatic compressibility $\kappa_S(\omega)$. **c**, The longitudinal expansion coefficient $\alpha_l(\omega)$, for which data were measured in the time domain and subsequently converted to the frequency representation by a numerical Laplace transform³⁴. **d**, The longitudinal heat capacity $c_l(\omega)$.

limited in some directions, leading to significant shear stresses in the sample³³. This implies that $c_p(\omega)$ is not measured directly; rather it is the ‘longitudinal’ dynamic heat capacity $c_l(\omega)$ that is measured in most experiments³³. Similarly for thermal expansion we measure the dynamic longitudinal expansion coefficient $\alpha_l(\omega)$, rather than the dynamic isobaric expansion coefficient $\alpha_p(\omega)$ (ref. 34,39). Fortunately, knowledge of the shear modulus $G(\omega)$ allows one to calculate $c_p(\omega)$ and the isobaric expansion coefficient $\alpha_p(\omega)$ from data (see equation (2) below). In summary, to determine the predicted density-scaling exponent γ_{isom} we measured the following four complex linear thermoviscoelastic response functions: the dynamic adiabatic compressibility $\kappa_S(\omega)$, the dynamic longitudinal heat capacity $c_l(\omega)$, the dynamic longitudinal expansion coefficient $\alpha_l(\omega)$, and the dynamic shear modulus $G(\omega)$.

The dynamic shear modulus $G(\omega)$ was measured using a piezoceramic transducer³⁵, the dynamic adiabatic compressibility $\kappa_S(\omega)$ by a similar technique³⁶, and the dynamic longitudinal heat capacity $c_l(\omega)$ was measured using the 3 ω -method³⁷ in a spherical geometry³⁸. The dynamic longitudinal expansion coefficient $\alpha_l(\omega)$

was calculated by Laplace transformation of a signal measured in the time domain using capacitive dilatometry^{34,39} (more details on the methods are given in the Methods section).

Examples of the measured complex, dynamic linear-response functions are shown in Fig. 2. In principle, we need only data at one state point to determine γ_{isom} from equation (1). In practice, we used several temperatures to estimate reliably the temperature dependence of the short-time and long-time levels. This was done to be able to extrapolate the DC704 expansion coefficient, which was obtained at lower temperatures than the other response functions (see the Methods section). The temperature 214 K is close to the calorimetric glass transition temperature of DC704, but it should be emphasized that all measurements refer to the linear response of the equilibrium liquid, a state that needs careful annealing to be reached, particularly at our lowest temperatures. The relevant values of $\beta_V(\omega)$ and $c_V(\omega)$ were calculated from the high- and low-frequency limits of the four measured thermoviscoelastic response functions, respectively, by solving the following four equations^{33,34,38,39} with four unknowns:

$$c_l(\omega) = \frac{1 + (4/3)G(\omega)\kappa_S(\omega)}{1 + (4/3)G(\omega)\kappa_T(\omega)} c_p(\omega)$$

$$\alpha_l(\omega) = \frac{\alpha_p(\omega)}{1 + (4/3)G(\omega)\kappa_T(\omega)}$$

$$c_V(\omega) = c_p(\omega) - \frac{T(\alpha_p(\omega))^2}{\kappa_T(\omega)} \quad (2)$$

$$\kappa_S(\omega) = \frac{c_V(\omega)\kappa_T(\omega)}{c_p(\omega)}$$

and using the relation $\beta_V(\omega) = \alpha_p(\omega)/\kappa_T(\omega)$. The values of the measured short- and long-time levels at the reference temperature are reported in Table 1. When substituted into equation (1) we find that the isomorph prediction for the density-scaling exponent is $\gamma_{\text{isom}} = 6 \pm 2$, which is in good agreement with the experimental density-scaling exponent $\gamma_{\text{scale}} = 6.2 \pm 0.2$ (Fig. 1b). The large uncertainty of γ_{isom} derives from the fact that measuring the absolute values of the frequency-dependent thermoviscoelastic response functions is very challenging. Even considering the large uncertainty in the predicted γ_{isom} , it is striking that γ_{isom} agrees with the exponent from density scaling. This agreement shows that for DC704 thermoviscoelastic linear-response measurements at one ambient-pressure state point can be used to predict the density-scaling exponent, which describes the density and temperature dependence of relaxation times varying from micro- to kilo-seconds, measured at pressures up to 400 MPa over a 90 K temperature range. This is a main conclusion of the present paper.

The correlation coefficient between W and U in the NVT ensemble,

$$R = \frac{\langle \Delta W \Delta U \rangle}{\sqrt{\langle (\Delta U)^2 \rangle \langle (\Delta W)^2 \rangle}}$$

measures how strong the virial/potential energy correlations are in a liquid ($-1 \leq R \leq 1$; the closer R is to unity, the better correlation). It therefore provides a measure of how well a liquid is expected to follow the isomorph theory. Expressing R in terms of linear-response functions, it becomes clear that R is given directly by the linear NVT Prigogine–Defay (PD) ratio⁶, $\Pi_{\text{VT}}^{\text{lin}}$:

$$R = \frac{\beta_V^{\text{slow}} - \beta_V^{\text{fast}}}{\sqrt{-(K_T^{\text{slow}} - K_T^{\text{fast}})(c_V^{\text{slow}} - c_V^{\text{fast}})/T}} = \frac{1}{\sqrt{\Pi_{\text{VT}}^{\text{lin}}}}$$

Here $K_T = 1/\kappa_T$ is the isothermal bulk modulus. The PD ratio equals unity if the liquid is a single-parameter liquid^{7–15}. Thus, a perfectly correlating liquid is what was traditionally referred to as

Table 1 | Measured short-time ('fast') and long-time ('slow') levels of the four thermoviscoelastic response functions of DC704 at 214 K.

	DC704 (214 K)
$c_f^{\text{slow}} [10^6 \text{J} (\text{K m}^3)^{-1}]$	1.65 ± 0.15
$c_f^{\text{fast}} [10^6 \text{J} (\text{K m}^3)^{-1}]$	1.35 ± 0.05
$\kappa_S^{\text{slow}} [10^{-9} \text{Pa}^{-1}]$	0.25 ± 0.03
$\kappa_S^{\text{fast}} [10^{-9} \text{Pa}^{-1}]$	0.19 ± 0.03
$\alpha_f^{\text{slow}} [10^{-3} \text{K}^{-1}]$	0.46 ± 0.04
$\alpha_f^{\text{fast}} [10^{-3} \text{K}^{-1}]$	0.11 ± 0.01
$G^{\text{slow}} [10^9 \text{Pa}]$	0
$G^{\text{fast}} [10^9 \text{Pa}]$	1.1 ± 0.05
$\Pi_{\text{pT}}^{\text{lin}}$	1.1 ± 0.3
$\Pi_{\text{VT}}^{\text{lin}}$	1.2 ± 0.6
R	0.9 ± 0.2
γ_{isom}	6 ± 2
γ_{scale}	6.2 ± 0.2

These data were used to calculate the exponent γ_{isom} predicted to be equal to γ_{scale} . The error bars on the measured data reflect max-min values, the errors bars on the calculated values were identified using standard error propagation techniques.

a single-parameter liquid⁶. Earlier studies of the PD ratio gave no physical interpretation of values different from one, even if these were close to one. The above interpretation of the linear NVT PD ratio as given by the correlation coefficient shows that the PD ratio provides a measure of how strongly correlating a given liquid is.

When the linear NVT PD ratio is exactly unity, other linear PD ratios, for example, the experimentally relevant linear NpT PD ratio, are also unity⁶. When $\Pi_{\text{pT}}^{\text{lin}}$ is not strictly one, there is no such result, but by continuity we surmise that $\Pi_{\text{pT}}^{\text{lin}}$ is close to unity if and only if $\Pi_{\text{VT}}^{\text{lin}}$ is. For DC704 we find $\Pi_{\text{pT}}^{\text{lin}} = 1.1 \pm 0.3$ and $\Pi_{\text{VT}}^{\text{lin}} = 1.2 \pm 0.6$, which is consistent with this conjecture.

Whereas neither the linear NVT PD ratio nor the linear NpT PD ratio have been reported in the literature before this study, there are many reports on the classical (NpT) PD ratio. This quantity is calculated using temperature-extrapolated liquid and glassy static responses, where the glassy response is defined from the low-temperature ($T < T_g$) solid response:

$$\Pi_{\text{pT}}^{\text{classic}} \equiv \frac{(\kappa_T^{\text{liq}}(T_g) - \kappa_T^{\text{glass}}(T_g))(c_p^{\text{liq}}(T_g) - c_p^{\text{glass}}(T_g))}{T_g(\alpha_p^{\text{liq}}(T_g) - \alpha_p^{\text{glass}}(T_g))^2}$$

Here ' T_g ' indicates the extrapolation to the glass transition temperature. The classical PD ratio involves extrapolations and is therefore not rigorously well-defined^{6,10,40,41}. Moreover, the glassy response depends on how the glass is made (for example, the cooling rate), which means that different protocols might well result in somewhat different values of the PD ratio. Nevertheless, the classical PD ratio provides an experimentally much easier route for estimating the degree of *WU* correlation than measuring the proper frequency-dependent linear thermoviscoelastic response functions at one temperature. In the absence of linear PD ratio data we compiled all the literature data we could find on the classical PD ratio.

Figure 3 shows the PD values for 22 glass formers, including polymers, a metallic alloy, inorganic and molecular liquids (both hydrogen-bond rich and van der Waals bonded). The systems have been sorted according to their PD ratio. In analogy with the NVT case, we define an approximate correlation coefficient

of the NpT ensemble as the inverse square root of the NpT PD ratio. Network-bonded inorganic glass formers such as silica glasses and hydrogen-bond rich molecular liquids (for example, glycerol and glucose) have large PD ratios. In contrast, van der Waals systems, exemplified by the polymers and the two mixtures with *o*-terphenyl as the major constituent, have PD ratios close to one. This confirms the conjecture that van der Waals liquids are strongly correlating, whereas associated and network-forming liquids are not^{4,5}. It is also interesting to compare propanol and glycerol, which have the same backbone of three carbon atoms, but one and three hydroxyl groups, respectively. Propanol, with only one hydroxyl group and therefore fewer hydrogen bonds, has a smaller PD ratio than glycerol. The pattern in Fig. 3 is consistent with computer simulation results, where liquids without directional bonding or competing interactions are generally found to be strongly correlating^{4,5}.

The glassy and liquid extrapolated response values used to calculate the classical PD ratio provide an alternative, but less well-defined way of calculating γ_{isom} (this type of expression for γ_{scale} was also found in ref. 31 by using an entropy-based model for the dynamics). We did the analysis on the data of a mixture of 67% *o*-terphenyl and 33% *o*-phenylphenol from a paper by Takahara and co-workers⁴². This mixture is a strongly correlating liquid with $\Pi_{\text{pT}}^{\text{classic}} = 1.20$ (ref. 42). We find $\gamma_{\text{isom}} = 5.4 \pm 1$, which is to be compared to the (absolute-unit) density scaling exponent for this liquid $\gamma_{\text{scale}} = 6.2 \pm 0.2$ (ref. 24). This is consistent with the isomorph prediction (see the Supplementary Information for details).

We have argued that the PD ratio of a large class of liquids should be regarded as essentially equal to unity. The general consensus, however, is that unity PD ratios are rare exceptions or not allowed (see, for example, refs 42–44). In recent years, several studies have been dedicated to understanding non-unity PD ratios. These approaches can be summarized as follows: (1) Linear-response theories of thermoviscoelasticity yielding non-unity ratios for systems with more than one internal state variable^{6,13,45,46}. (2) A non-equilibrium thermodynamic theory explaining non-unity of the classical PD ratio as a non-equilibrium effect (even in the case of a single internal state variable)⁴³. (3) A Landau theory using nano-thermodynamics where dynamical heterogeneity is the origin of non-unity PD ratios⁴⁷. In this paper we adopted the first viewpoint, which is the original rigorous linear PD ratio interpretation going back to the seminal works by Moynihan and co-workers more than 30 years ago^{10,48}.

Our findings show that strongly correlating liquids exist not merely in computer simulations, but also as real liquids. These liquids are simpler than liquids in general, while still having all the hallmarks of viscous slowing down on supercooling, eventually leading to a glass transition. For strongly correlating liquids there is an 'isomorph filter'⁵ according to which theories for the non-Arrhenius temperature dependence of the relaxation time can be sorted: only theories that express the relaxation time in terms of an isomorph invariant can be correct for strongly correlating liquids and thus be of general validity. Moreover, for strongly correlating liquids several phenomena can be explained in simple terms on the basis of the existence of isomorphs in the liquid's phase diagram⁵. Examples include isochronal superposition (that is, the finding that dielectric loss spectra under varying pressure and temperature are invariant for states with the same relaxation time), and ageing behaviour after temperature and density jumps^{5,49}. These phenomena are well understood for perfectly correlating liquids, and liquids with strong correlations inherit the behaviour to a good approximation. The degree to which these phenomena survive as the correlation gets poorer is a cardinal point for further research; it is likely that some predictions are more sensitive to deviations from perfect correlation than others. We suggest that perfectly correlating liquids should be regarded as 'ideal gas' or 'Ising models'

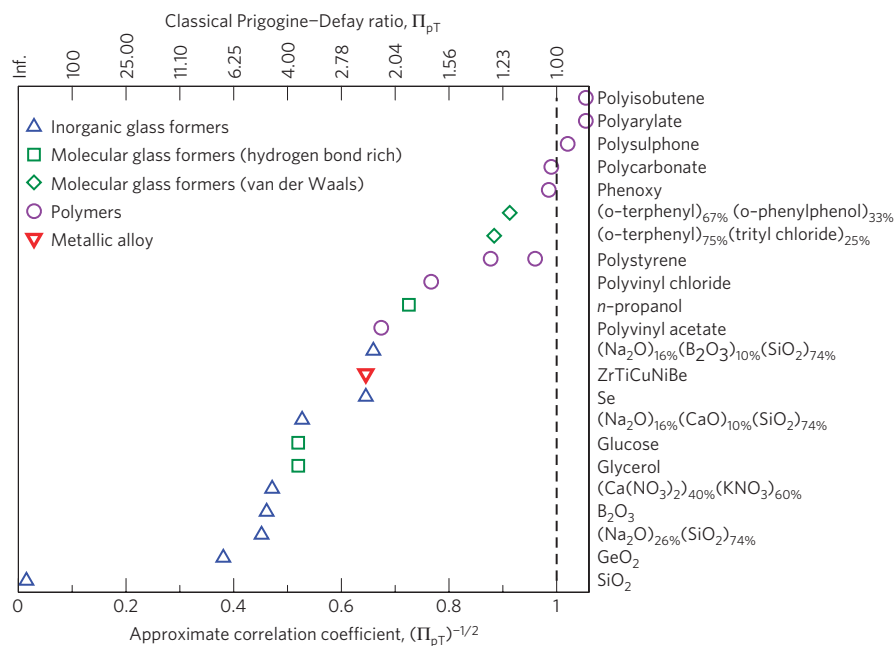


Figure 3 | Literature values of the classical (NpT) Prigogine-Defay (PD) ratios $\Pi_{pT}^{\text{classic}}$ of 22 glass formers. The liquids, which are sorted according to reported value of the PD ratio, include inorganic glass formers (triangles pointing up), hydrogen-bond-rich molecular liquids (squares), van der Waals molecular liquids (diamonds), polymers (circles), and a metallic alloy (triangle pointing down). The inverse square root of the classical NpT Prigogine-Defay ratio gives an estimate for the correlation coefficient (lower x-axis). Strong correlations are found in van der Waals bonded molecular liquids and polymers (the Supplementary Information provides the PD values shown in the figure and relevant references; note that each symbol in the figure corresponds to the liquid listed to the right).

of liquids—that is, simple systems for which a number of generic features of the glass transition phenomenology can be understood. In this way, the identification of what constitutes a ‘simple’ liquid will hopefully lead to a better general understanding of viscous liquids and the glass transition.

Methods

The liquid studied, the Dow Corning diffusion pump silicone oil tetramethyl-tetraphenyl-trisiloxane DC704, was used as received without further purification. The different measurements (in total six different experiments) were performed on a sample taken from the same bottle. DC704 is not hygroscopic so water contamination is not a problem. Moreover, the pVT measurements and the high pressure dielectric spectroscopy measurements used to determine γ_{scale} were performed in the same lab and by the same team. For all these reasons we are fairly confident by the γ_{scale} of DC704 reported in the paper; the uncertainties are much larger for γ_{isom} .

The four thermoviscoelastic linear-response techniques use a custom-built cryostat⁵⁰. $G(\omega)$, $\kappa_S(\omega)$ and $c_l(\omega)$ were measured in the same cryostat; $\alpha_l(\omega)$ was obtained from measurements in the same type of cryostat and the temperatures were calibrated with dielectric spectra taken on the DC704 sample, ensuring that the absolute temperature calibration was the same for all types of measurements.

The shear modulus $G(\omega)$ is measured over the frequency range 10^{-3} – 10^4 Hz (ref. 35), and the adiabatic compressibility $\kappa_S(\omega)$ is measured over 10^{-2} – 10^4 Hz (ref. 36). Both methods are optimized for measurements on very stiff materials (modulus ranges of MPa–GPa) and are based on piezoceramic materials that act as converters of mechanical properties into electrical properties.

The measurements of specific heat were done using a 3ω thermal-effusion method in a spherical geometry³⁸, a technique which is equivalent to the planar plate 3ω technique of Birge and Nagel³⁷, however using a spherical thermistor bead instead of a thin planar metal film. It covers a frequency range of $10^{-2.5}$ – $10^{0.5}$ Hz, limited by the intrinsic frequency dependence of the thermal impedance in this geometry. The isobaric specific heat, $c_p(\omega) = (\kappa_T(\omega)/\kappa_S(\omega))c_V(\omega)$ is not measured in this geometry; rather what is measured is the longitudinal specific heat, $c_l(\omega) = (M_S(\omega)/M_T(\omega))c_V(\omega)$ (where $M(\omega)$ represents longitudinal moduli)³⁸.

The measurements of the longitudinal thermal expansion coefficient in the time domain $\alpha_l(t)$ were carried out using a microregulator^{34,50}, allowing for fast temperature changes of a small planar capacitor. This technique is based on a temperature-step variant of ‘capacitive scanning dilatometry’³⁹, which uses the fact that the capacitance of a capacitor is inversely proportional to the thickness of the liquid in the capacitor. What is measured in this geometry is the longitudinal thermal expansion coefficient^{34,39} α_l (see equation (2); ref. 33 for a derivation). The

dynamic longitudinal expansion coefficient $\alpha_l(\omega)$ shown in Fig. 2 was calculated by Laplace transformation of a signal measured in the time domain. However, equation (1) requires only knowledge of the high and low-frequency limits of the response functions and the required limits for $\alpha_l(\omega)$ were obtained directly from the data measured in the time domain (as short and long-time limits respectively), that is, without a Laplace transformation.

The heat capacity is the response function for which data are measured over the narrowest frequency (and therefore also temperature) range. The studied temperature range was 214–218 K, and within the experimental uncertainties there is no temperature dependence of the slow and fast values. We chose 214 K as the reference temperature to minimize the extrapolation required of the expansion coefficient data, which were measured in the 204–210 K range.

All data were taken in thermal equilibrium, a state it takes careful annealing to reach at low temperatures.

Received 20 December 2010; accepted 25 May 2011; published online 3 July 2011

References

1. Debenedetti, P. G. Supercooled glassy water. *J. Phys. Condens. Matter* **15**, R1669–R1726 (2003).
2. Angell, C. A. Insights into phases of liquid water from study of its unusual glass-forming properties. *Science* **319**, 582–587 (2008).
3. Pedersen, U. R., Bailey, N. P., Schröder, T. B. & Dyre, J. C. Strong pressure–energy correlations in van der Waals liquids. *Phys. Rev. Lett.* **100**, 015701 (2008).
4. Schröder, T. B., Bailey, N. P., Pedersen, U. R., Gnan, N. & Dyre, J. C. Pressure–energy correlations in liquids. III. Statistical mechanics and thermodynamics of liquids with hidden scale invariance. *J. Chem. Phys.* **131**, 234503 (2009).
5. Gnan, N., Schröder, T. B., Pedersen, U. R., Bailey, N. P. & Dyre, J. C. Pressure–energy correlations in liquids. IV. ‘‘Isomorphs’’ in liquid phase diagrams. *J. Chem. Phys.* **131**, 234504 (2009).
6. Ellegaard, N. L. *et al.* Single-order-parameter description of glass-forming liquids: A one-frequency test. *J. Chem. Phys.* **126**, 074502 (2007).
7. Davies, R. O. & Jones, G. O. Thermodynamic and kinetic properties of glasses. *Adv. Phys.* **2**, 370–410 (1953).
8. Prigogine, I. & Defay, R. *Chemical Thermodynamics* (Longmans Green and Co., 1954).
9. Goldstein, M. Some thermodynamic aspects of the glass transition: Free volume, entropy, and enthalpy theories. *J. Chem. Phys.* **39**, 3369–3374 (1963).

10. Moynihan, C. T. & Gupta, P. K. Order parameter model for structural relaxation in glass. *J. Non-Cryst. Solids* **29**, 143–158 (1978).
11. Berg, J. I. & Cooper, A. R. Linear non-equilibrium thermodynamic theory of glass-transition kinetics. *J. Chem. Phys.* **68**, 4481–4485 (1978).
12. Hodge, I. M. Enthalpy relaxation and recovery in amorphous materials. *J. Non-Cryst. Solids* **169**, 211–266 (1994).
13. Nieuwenhuizen, Th. M. Ehrenfest relations at the glass transition: Old to a new paradox. *Phys. Rev. Lett.* **79**, 1317–1320 (1997).
14. Wondraczek, L., Krolikowski, S. & Behrens, H. Relaxation and Prigogine–Defay ratio of compressed glasses with negative viscosity–pressure dependence. *J. Chem. Phys.* **130**, 204506 (2009).
15. Lion, A. & Peters, J. Coupling effects in dynamic calorimetry: Frequency-dependent relations for specific heat and thermomechanical responses—a one-dimensional approach based on thermodynamics with internal state variables. *Thermochim. Acta* **500**, 76–78 (2010).
16. Angell, C. A., Ngai, K. L., McKenna, G. B., McMillan, P. F. & Martin, S. W. Relaxation in glass-forming liquids and amorphous solids. *J. Appl. Phys.* **88**, 3113–3157 (2000).
17. Dyre, J. C. The glass transition and elastic models of glass-forming liquids. *Rev. Mod. Phys.* **78**, 953–972 (2006).
18. Cavagna, A. Supercooled liquids for pedestrians. *Phys. Rep.* **476**, 51–124 (2009).
19. Floudas, G., Paluch, M., Grzybowski, A. & Ngai, K. L. *Molecular Dynamics of Glass-Forming Systems* (Advances in Dielectrics, Springer, 2010).
20. Berthier, L., Biroli, G., Bouchaud, J.-P., Cipelletti, L. & van Saarloos, W. (eds). *Dynamical heterogeneities in glasses, colloids, and granular media*. Oxford Univ. Press (in the press).
21. Alba-Simionesco, C., Cailliaux, A., Alegria, A. & Tarjus, G. Scaling out the density dependence of the α relaxation in glass-forming polymers. *Europhys. Lett.* **68**, 58–64 (2004).
22. Dreyfus, C., Le Grand, A., Gapinski, J., Steffen, W. & Patkowski, A. Scaling the α -relaxation time of supercooled fragile organic liquids. *Eur. Phys. J. B* **42**, 309–319 (2004).
23. Casalini, R. & Roland, C. M. Thermodynamical scaling of the glass transition dynamics. *Phys. Rev. E* **69**, 062501 (2004).
24. Roland, C. M., Hensel-Bielowka, S., Paluch, M. & Casalini, R. Supercooled dynamics of glass-forming liquids and polymers under hydrostatic pressure. *Rep. Prog. Phys.* **68**, 1405–1478 (2005).
25. Ferrer, M. L. *et al.* Supercooled liquids and the glass transition: Temperature as the control variable. *J. Chem. Phys.* **109**, 8010–8015 (1998).
26. Roland, C. M. Relaxation phenomena in vitrifying polymers and molecular liquids. *Macromol* **43**, 7875–7890 (2010).
27. Bridgman, P. W. Viscosities to 30,000 kg/cm². *Proc. Am. Acad. Arts Sci.* **77**, 117–128 (1949).
28. Roland, C. M., Casalini, R., Bergman, R. & Mattsson, J. Role of hydrogen bonds in the supercooled dynamics of glass-forming liquids at high pressures. *Phys. Rev. B* **77**, 012201 (2008).
29. Coslovich, D. & Roland, C. M. Density scaling in viscous liquids: From relaxation times to four-point susceptibilities. *J. Chem. Phys.* **131**, 151103 (2009).
30. Schröder, T. B., Pedersen, U. R., Bailey, N. P., Toxvaerd, S. & Dyre, J. C. Hidden scale invariance in molecular van der Waals liquids: A simulation study. *Phys. Rev. E* **80**, 041502 (2009).
31. Casalini, R., Mohanty, U. & Roland, C. M. Thermodynamic interpretation of the scaling of the dynamics of supercooled liquids. *J. Chem. Phys.* **125**, 014505 (2006).
32. de Groot, S. R. & Mazur, P. *Non-Equilibrium Thermodynamics* (North-Holland, Amsterdam, 1962).
33. Christensen, T., Olsen, N. B. & Dyre, J. C. Conventional methods fail to measure $c_p(\omega)$ of glass-forming liquids. *Phys. Rev. E* **75**, 041502 (2007).
34. Niss, K., Christensen, T. & Dyre, J. C. Measuring the dynamic thermal expansivity of molecular liquids near the glass transition. Preprint at <http://arXiv.org/abs/1103.4104> (2011).
35. Christensen, T. & Olsen, N. B. A rheometer for the measurement of a high shear modulus covering more than seven decades of frequency below 50 kHz. *Rev. Sci. Instrum.* **66**, 5019–5031 (1995).
36. Christensen, T. & Olsen, N. B. Determination of the frequency-dependent bulk modulus of glycerol using a piezoelectric spherical shell. *Phys. Rev. B* **49**, 15396–15399 (1994).
37. Birge, N. O. & Nagel, S. R. Specific-heat spectroscopy of the glass-transition. *Phys. Rev. Lett.* **54**, 2674–2677 (1985).
38. Jakobsen, B., Olsen, N. B. & Christensen, T. Frequency-dependent specific heat from thermal effusion in spherical geometry. *Phys. Rev. E* **81**, 061505 (2010).
39. Bauer, C. *et al.* Capacitive scanning dilatometry and frequency-dependent thermal expansion of polymer films. *Phys. Rev. E* **61**, 1755–1764 (2000).
40. Roe, R. J. Thermodynamics of glassy state with multiple order parameters. *J. Appl. Phys.* **48**, 4085–4091 (1977).
41. Moynihan, C. T. & Lesikar, A. V. Comparison and analysis of relaxation processes at the glass-transition temperature. *Ann. N.Y. Acad. Sci.* **371**, 151–169 (1981).
42. Takahara, S., Ishikawa, M., Yamamuro, O. & Matsuo, T. Structural relaxations of glassy polystyrene and o-terphenyl studied by simultaneous measurement of enthalpy and volume under high pressure. *J. Phys. Chem. B* **103**, 792–796 (1999).
43. Schmelzer, J. W. P. & Gutzow, I. The Prigogine–Defay ratio revisited. *J. Chem. Phys.* **125**, 184511 (2006).
44. Banerjee, R., Modak, S. K. & Samanta, S. Glassy phase transition and stability in black holes. *Eur. Phys. J. C* **70**, 317–328 (2010).
45. Pick, R. M. The Prigogine–Defay ratio and the microscopic theory of supercooled liquids. *J. Chem. Phys.* **129**, 124115 (2008).
46. Lieb, C., Lion, A., Kolmeder, S. & Peters, J. Representation of the glass-transition in mechanical and thermal properties of glass-forming materials: A three-dimensional theory based on thermodynamics with internal state variables. *J. Mech. Phys. Solids* **58**, 1338–1360 (2010).
47. Javaheri, M. R. H. & Chamberlin, R. V. A free-energy landscape picture and Landau theory for the dynamics of disordered materials. *J. Chem. Phys.* **125**, 154503 (2006).
48. Lesikar, A. V. & Moynihan, C. T. Some relations connecting volume and enthalpy relaxation in the order parameter model of liquids and glasses. *J. Chem. Phys.* **72**, 6422–6423 (1980).
49. Gnan, N., Maggi, C., Schroder, T. B. & Dyre, J. C. Predicting the effective temperature of a glass. *Phys. Rev. Lett.* **104**, 125902 (2010).
50. Igarashi, B. *et al.* A cryostat and temperature control system optimized for measuring relaxations of glass-forming liquids. *Rev. Sci. Instrum.* **79**, 045105 (2008).

Acknowledgements

The Centre for Viscous Liquid Dynamics ‘Glass and Time’ is sponsored by the Danish National Research Foundation (DNRF). Work at NRL is supported by Office of Naval Research. URP is supported by The Danish Council for Independent Research in Natural Sciences.

Author contributions

U.R.P. and K.N. conceived the project. D.G., U.R.P., B.J., J.C.D. and K.N. wrote the paper with input from C.M.R. D.G., U.R.P., and K.N. did the main data analysis. T.H. measured the shear modulus and compressibility and did the raw data analysis. B.J. and T.C. measured the heat capacity and did the raw data analysis. K.N. measured the expansion coefficient and did the raw data analysis. T.C. and N.B.O. conceived and developed the four thermoviscoelastic measuring techniques used. D.G., D.F. and R.C. measured the high-pressure data and did the scaling data analysis. U.R.P., N.P.B., T.C., T.B.S. and J.C.D. supplied the theoretical background for the project, which was coordinated by K.N.

Additional information

The authors declare no competing financial interests. Supplementary information accompanies this paper on www.nature.com/naturephysics. Reprints and permissions information is available online at <http://www.nature.com/reprints>. Correspondence and requests for materials should be addressed to K.N.